Cylindrical lateral depth-sensing indentation testing of thin anisotropic elastic films

Argatov, I. I.; Mishuris, G. S.; Paukshto, M. V.

Published in:
European Journal of Mechanics - A/Solids

DOI:
10.1016/j.euromechsol.2014.07.009

Publication date:
2015

Citation for published version (APA):
Argatov, I. I., Mishuris, G. S., & Paukshto, M. V. (2015). Cylindrical lateral depth-sensing indentation testing of thin anisotropic elastic films. *European Journal of Mechanics - A/Solids*, *49*, 299-307. https://doi.org/10.1016/j.euromechsol.2014.07.009

Cylindrical lateral depth-sensing indentation testing of thin anisotropic elastic films

I.I. Argatov [a,*], G.S. Mishuris [b], M.V. Paukshto [c],

[a] *Engineering Mechanics Laboratory, University of Oulu, 90014 Oulu, Finland*

[b] *Institute of Mathematics and Physics, Aberystwyth University, Ceredigion SY23 3BZ, Wales, UK*

[c] *Fibralign Corp, 32930 Alvarado-Niles Rd., Union City, CA 94587, USA*

Abstract

A two-dimensional frictionless contact problem for a parabolic indenter pressed against an orthotropic elastic strip resting on a frictionless rigid substrate is studied. The sixth-order asymptotic solution is obtained in the case of a relatively small contact zone with respect to the elastic strip thickness. The so-called cylindrical lateral indentation test, which utilizes lateral contact of a cylindrical indenter, is developed for indentation testing of a thin transversely isotropic film with the symmetry plane orthogonal to the contact plane under the assumption that the film thickness is small compared to the cylinder indenter length. The presented testing methodology is based on a least squares best fit of the second-order asymptotic model to the depth-sensing indentation data.

Key words: Indentation testing, transversely isotropic, thin layer, asymptotic model

1 Introduction

Indentation tests have been shown to be useful both in assessing viability of biological tissues (such as articular cartilage (Korhonen et al., 2003)) and identification of their mechanical properties (Dimitriadis et al., 2002). In recent years, the atomic force microscopy (AFM) indentation has become an important technique for quantifying the mechanical properties of soft polymers (Liao et al., 2010) and biological materials (Stolz et al., 2009).

It is well known (Pandolfi and Vasta, 2012) that many biological materials are characterized by anisotropy. Moreover, most load-bearing tissues like heart, ligament, and blood

* Corresponding author.

Email addresses: ivan.argatov@oulu.fi (I.I. Argatov), ggm@aber.ac.uk (G.S. Mishuris), mpaukshto@fibralignbio.com (M.V. Paukshto).

vessels are highly anisotropic, and the underlying structure is distinct and essential for function. The dependence of elastic moduli on the orientation in such a tissue is often determined by the orientation of collagen fibrils. For example, transverse isotropy is observed in nanofibrillar collagen scaffold (see Fig. 1) that mimic the structure of collagen organization in blood vessels (Huang et al., 2013).

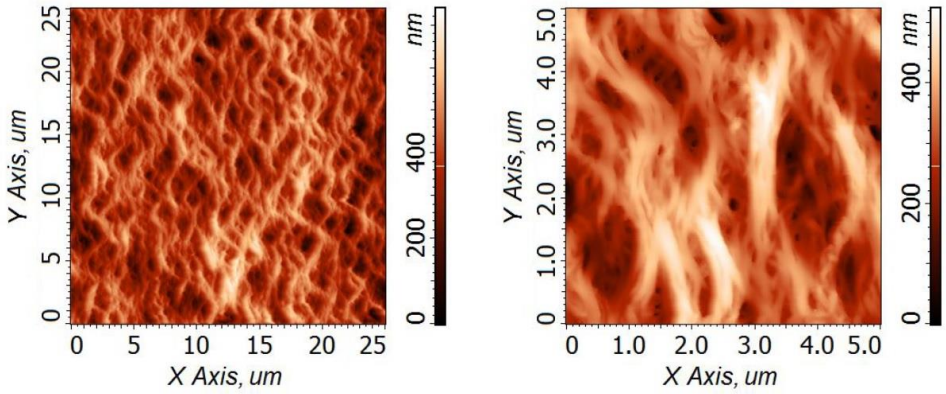

Figure 1. AFM images of aligned-braided collagen matrix at two magnifications.

Mechanical properties of small specimens of soft materials can be determined by depth-sensing indentation technique (Fischer-Cripps, 2004) based on the load-depth data of the entire loading protocol. In particular, flat-ended cylindrical (Choi et al., 2008), spherical (Dimitriadis et al., 2002), conical (Pelletier et al., 2006), and pyramidal (Borodich et al., 2003; Giannakopoulos, 2006) indenters are widely used, and the corresponding analytical or numerical solutions are employed. Implicit methods to determine the indentation modulus of anisotropic materials with spherical and flat-ended cylinder indenters originate from the pioneering work of Willis (1966, 1967) and Vlassak and Nix (1993, 1994), who simplified Willis' solution and provided implicit solution schemes for other indenter shapes. In particular, a Rayleigh–Ritz approximation to the contact area and the load-indentation relation was developed by Vlassak et al. (2003) to evaluate the equivalent indentation modulus by spherical and conical indenters. An explicit solution for the indentation moduli of a semi-infinite general orthotropic medium under conical indentation in the three principal material symmetry directions was proposed by Delafargue and Ulm (2004).

The majority of the available analytical solutions of contact problems were obtained for an isotropic elastic half-space or a transversely isotropic half-space with the plane of isotropy parallel to the contact plane (Sveklo, 1964; Ding et al., 2006). With respect to indentation testing of thin films, the thickness effect plays an important role in the accurate assessment of the film moduli (Hayes et al., 1972; Argatov et al., 2013; Argatov and Sabina, 2013). The transverse anisotropy of samples requires the development of novel analytical solutions to address the thickness effect.

In the present work, we consider the so-called cylindrical lateral indentation test, which utilizes lateral contact of a cylindrical indenter (see Fig. 2). Such a test can be approximately modeled in the framework of the two-dimensional contact model for an orthotropic elastic strip. It should be mentioned that in contrast to the three-dimensional Hertzian theory, which provides a complete solution of the indentation problem for an elastic half-space and a paraboloidal indenter, the two-dimensional Hertzian contact theory, being applied

to an elastic half-plane and a rigid parabolic indenter, does not allow to determine the indenter displacement. This paradox was resolved in the framework of asymptotic modeling approach (Argatov, 2001). Namely, because of the finite thickness of the anisotropic coating, it is possible to derive asymptotic expressions for the indenter displacement.

Recently, Batra and Jiang (2008) have reviewed the state-of-the-art in analytical solutions of contact problems for anisotropic materials. Using Stroh's formalism, they studied the two-dimensional indentation problem for an anisotropic elastic layer. Very recently, Greenwood and Barber (2012) reconsidered the two-dimensional contact problem for a parabolic (cylindrical) indenter and an isotropic elastic layer by utilizing Green's function approach. A two-dimensional contact problem for an orthotropic elastic strip and a parabolic indenter was studied in (Aleksandrov, 2006; Erbaş et al., 2011) by asymptotic methods. Here we extend the previous asymptotic analysis and employ the results obtained in the development of the depth-sensing indentation test. Novelty of the presented asymptotic approach is based on the method of integral characteristics of the contact pressure distribution previously developed (Argatov and Sabina, 2013) in the three-dimensional case and, in view of the specificity of the two-dimensional case, additionally utilizes the orthogonality property of the Chebyshev polynomials.

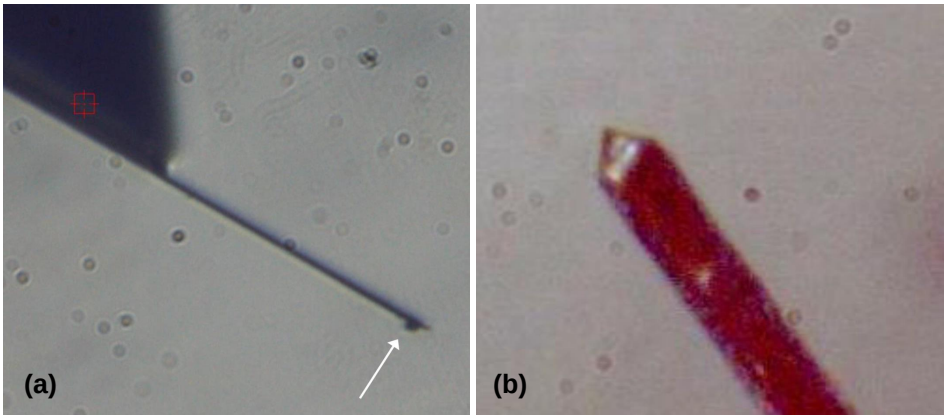

Figure 2. Pictures of a glass cylinder attached to the AFM cantilever: (a) side view; (b) bottom view. The glass cylinder length and diameter are about 18 μm and 6 μm, respectively.

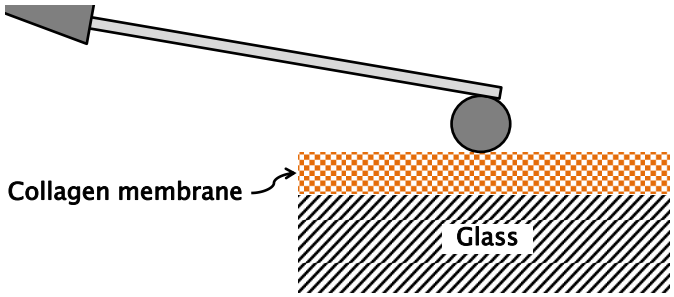

Figure 3. Indentation testing setup. Side view. Glass substrate with collagen coating; fibril direction is along the cylinder axis.

It is important to note that the employed asymptotic approach assumes that the film thickness h and the indenter radius, R, should be small compared to the cylinder indenter length, l, in order to apply a two-dimensional approximation for the stress-strain state beneath the indenter (see Fig. 4a). The case, when the indenter cylinder makes contact with an elastic half-space over a slender contact area (so that both inequalities $l \gg R$ and $h \gg l$ hold), was considered by Nayak and Johnson (1979) under the assumption

that the pressure distribution is semi-elliptical in the transverse direction. On the other hand, in order to apply a perturbation technique for solving the indentation problem, the contact zone size, a, is assumed to be small compared to the elastic film thickness, h, (see Fig. 4b).

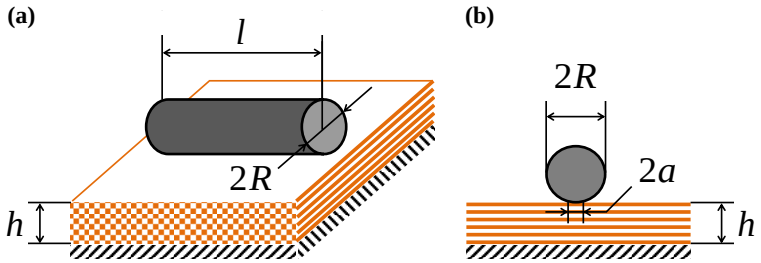

Figure 4. Details of dimensions and assumptions of smallness: (a) Ratios R/l and h/l are supposed to be small; (b) Ratio a/h is supposed to be small.

The rest of the paper is organized as follows. In Section 2, a governing integral equation of the two-dimensional indentation problem for an orthotropic elastic strip is formulated based on the previously obtained results of Aleksandrov (2006). In Section 3, following Argatov and Sabina (2013), we develop a new asymptotic method for solving the unilateral contact problem for a parabolic indenter with a priori unknown contact zone. The new results, in particular, are obtained with respect to the displacement-force relationship in Section 4. In Section 5, we actually consider the indentation test and outline the corresponding anisotropic materials properties evaluation procedure. Finally, in Section 7, we present a discussion of the results obtained and formulate our conclusions.

2 Indentation problem formulation

Recall (Lekhnitskii, 1981) that Hooke's law for a transversely isotropic material can be written as

$$\begin{aligned}
\varepsilon_{11} &= \frac{1}{E}(\sigma_{11} - \nu\sigma_{22}) - \frac{\nu_{\|}}{E_{\|}}\sigma_{33}, \quad \varepsilon_{23} = \frac{1}{2G_{\|}}\sigma_{23}, \\
\varepsilon_{22} &= \frac{1}{E}(-\nu\sigma_{11} + \sigma_{22}) - \frac{\nu_{\|}}{E_{\|}}\sigma_{33}, \quad \varepsilon_{13} = \frac{1}{2G_{\|}}\sigma_{13}, \\
\varepsilon_{33} &= -\frac{\nu_{\|}}{E_{\|}}(\sigma_{11} + \sigma_{22}) + \frac{1}{E_{\|}}\sigma_{33}, \quad \varepsilon_{12} = \frac{1}{2G}\sigma_{12}.
\end{aligned} \tag{1}$$

Here, E and ν are Young's modulus and Poisson's ratio in the symmetry plane, $G = E/[2(1+\nu)]$ is the in-plane shear modulus, $E_{\|}$ is the longitudinal Young's modulus, and $\nu_{\|}$ is Poisson's ratio for loading in the longitudinal direction.

For the case of plane strain deformations in the x_1x_2-plane (see Fig. 6a), under the assumption that $\varepsilon_{13} = \varepsilon_{23} = \varepsilon_{33} = 0$, Eqs. (1) imply that

$$\varepsilon_{11} = \left(\frac{1}{E} - \frac{\nu_{\|}^2}{E_{\|}}\right)\sigma_{11} - \left(\frac{\nu}{E} + \frac{\nu_{\|}^2}{E_{\|}}\right)\sigma_{22}, \quad \varepsilon_{12} = \frac{1+\nu}{E}\sigma_{12},$$
$$\varepsilon_{22} = -\left(\frac{\nu}{E} + \frac{\nu_{\|}^2}{E_{\|}}\right)\sigma_{11} + \left(\frac{1}{E} - \frac{\nu_{\|}^2}{E_{\|}}\right)\sigma_{22}. \tag{2}$$

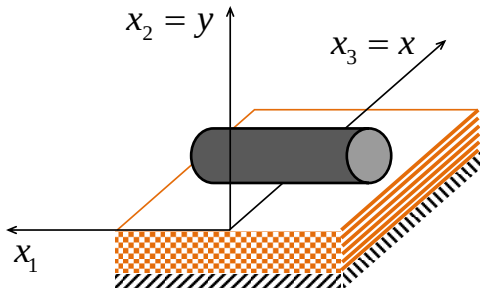

Figure 5. Glass substrate with collagen coating; fibril direction is perpendicular to the cylinder axis.

For the case of plane strain deformations in the x_2x_3-plane (see Fig. 6b), from Eqs. (1) it follows that

$$\varepsilon_{xx} = \left(\frac{1}{E_{\|}} - \frac{E\nu_{\|}^2}{E'^2}\right)\sigma_{xx} - \frac{\nu_{\|}(1+\nu)}{E_{\|}}\sigma_{yy}, \quad \varepsilon_{xy} = \frac{1}{2G_{\|}}\sigma_{xy},$$
$$\varepsilon_{yy} = -\frac{\nu_{\|}(1+\nu)}{E_{\|}}\sigma_{xx} + \frac{1-\nu^2}{E}\sigma_{yy}. \tag{3}$$

Equations (2) and (3) correspond to the longitudinal and transverse orientations of the indenter, respectively.

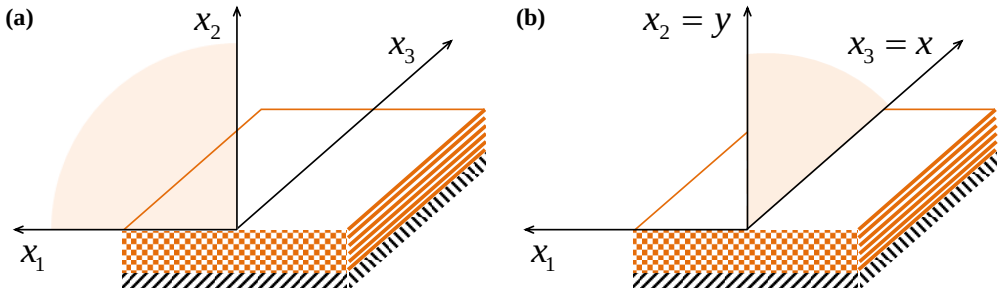

Figure 6. Coordinate system axes: (a) Plane of isotropy (transverse plane perpendicular to the longitudinal axis); (b) Longitudinal plane (plane perpendicular to the plane of isotropy).

Further, recall that the stress components can be expressed in terms of the Airy function as

$$\sigma_{xx} = \frac{\partial^2 U}{\partial y^2}, \quad \sigma_{yy} = \frac{\partial^2 U}{\partial x^2}, \quad \sigma_{xy} = -\frac{\partial^2 U}{\partial x \partial y}.$$

At that, the single deformation compatibility equation reduces to the following partial differential equation for the Airy function:

$$\frac{\partial^4 U}{\partial y^4} + 2A\frac{\partial^4 U}{\partial x^2 \partial y^2} + B\frac{\partial^4 U}{\partial x^4} = 0. \tag{4}$$

We consider two cases, which differ by the orientation of the indenter cylinder with respect to the longitudinal axis of the transversely isotropic material. Namely, in the longitudinal case the indenter cylinder is parallel to the axis of material symmetry, while in the transverse case it is parallel to the plane of isotropy and thus perpendicular to the material symmetry axis.

In the longitudinal and transverse cases, Eqs. (2) and (3), respectively, yield [1]

$$A^{||} = 1, \quad B^{||} = 1, \tag{5}$$

$$A^{\perp} = \frac{E_{\|}(E_{\|} - 2\nu_{\|}(1+\nu)G_{\|})}{2G_{\|}(E_{\|} - E\nu_{\|}^2)}, \quad B^{\perp} = \frac{E'^2(1-\nu^2)}{E(E_{\|} - E\nu_{\|}^2)}. \tag{6}$$

It is assumed that $A > 0$ and $B > 0$. Note also that the notation $A^{\|}$ and $B^{\|}$ is consistent with the notation $E_{\|}$ and reflects the orientation of the indenter cylinder to the axis of material symmetry.

In what follows, we consider a two-dimensional contact problem for an orthotropic elastic strip deposited on a rigid substrate. Under the assumption of frictionless contact between the elastic layer and the rigid substrate (i. e., $u_2 = 0$ and $\sigma_{12} = \sigma_{32} = 0$ at $x_2 = -h$) as well as between the elastic strip and a parabolic indenter, the two-dimensional contact problem can be reduced to the following integral equation (Aleksandrov, 2006):

$$\int\limits_{-a}^{a} q(x') K\Big(\frac{x'-x}{h}\Big)\, dx' = \pi\theta\Big(w - \frac{x^2}{2R}\Big), \quad |x| \le a. \tag{7}$$

Here, $q(x)$ is the contact pressure, w is the indenter displacement, a is the half-width of the contact area, which is a priori unknown, R is the radius of the cylindrical indenter, $K(t)$ is the kernel of the integral equation given by

$$K(t) = \int\limits_{0}^{\infty} \frac{L(u)}{u} \cos ut\, du. \tag{8}$$

In turn, the kernel function $L(u)$ and the elastic constant θ on the right-hand side of Eq. (7) are determined by the relation between the constants A and B, which enter Eqs. (4), as follows (Aleksandrov, 2006):

$$L_+(u) = \frac{\kappa_2 - \kappa_1}{\kappa_2 \operatorname{cth}(\kappa_1 u) - \kappa_1 \operatorname{cth}(\kappa_2 u)}, \quad \theta = \frac{\gamma\kappa_1\kappa_2}{\kappa_1 + \kappa_2} \quad (A^2 > B), \tag{9}$$

$$\kappa_{1,2} = \sqrt{A \pm \sqrt{A^2 - B}},$$

$$L_0(u) = \frac{\operatorname{ch}(2Au) - 1}{\operatorname{sh}(2Au) + 2Au}, \quad \theta = \frac{\gamma A}{2} \quad (A^2 = B), \tag{10}$$

$$L_-(u) = \frac{d[\operatorname{ch}(2cu) - \cos(2du)]}{d\operatorname{sh}(2cu) + c\sin(2du)}, \quad \theta = \frac{\gamma(c^2+d^2)}{2c} \quad (A^2 < B), \tag{11}$$

[1] The first formula (6) differs from the corresponding result obtained in (Aleksandrov, 2006), where G_{12} in formula (2.2) should be replaced with $2G_{12}$.

$$c = \frac{b}{\sqrt{2}}, \quad d = \frac{D}{\sqrt{2}b}, \quad D = \sqrt{B - A^2}, \quad b = \sqrt{A + \sqrt{A^2 + D^2}}.$$

At that, the elastic constant γ depends on the indenter orientation as

$$\gamma^{||} = \frac{EE_{\|}}{E_{\|} - E\nu_{\|}^2}, \quad \gamma^{\perp} = \frac{E}{1 - \nu^2}. \tag{12}$$

We emphasize that formulas (7) – (11) hold true for an orthotropic elastic strip under the appropriate choice of the elastic constants A and B.

Because transversely isotropic materials are characterized by five independent elastic constants (namely, E, $E_{\|}$, $G_{\|}$, ν, and $\nu_{\|}$), the transverse Young's modulus E , Poisson's ratios ν and $\nu_{\|}$, and two dimensionless ratios $E_{\|}/E$ and $G_{\|}/G = 2(1+\nu)G_{\|}/E$ will be regarded as primary elastic parameters.

The equilibrium equation gives

$$P = \mathcal{P}l, \quad \mathcal{P} = \int_{-a}^{a} q(x)\, dx, \tag{13}$$

where P is the contact force, l is the cylinder indenter length, $\mathcal{P} = P/l$ is the contact force per unit length.

Finally, the contact size parameter a should be determined from the condition that the contact pressure $q(x)$ vanishes at the end points $x = \pm a$ being positive inside the contact zone for $x \in (-a, a)$.

Note that the governing integral equation (7) is a Fredholm integral equation of the first kind, and its solvability was investigated in a number of studies (Vorovich et al., 1974; Erbaş et al., 2011). In the present paper, we obtain an asymptotic solution of Eq. (7) by utilizing integral characteristics of the kernel function (8). In particular, the sixth-order asymptotic solution is written out in the closed form.

3 Asymptotic solution for a relatively small contact zone

Under the assumption that the size of the contact zone is small compared to the layer thickness, an asymptotic solution can be based on the following expansion (Aleksandrov, 2006; Vorovich et al., 1974):

$$K(t) = -\ln t - \sum_{n=0}^{\infty} d_n t^{2n}. \tag{14}$$

Here the coefficients d_n are given by

$$d_0 = \int_0^{\infty} \frac{1 - L(u) - e^{-u}}{u} du, \tag{15}$$

$$d_n = \frac{(-1)^n}{(2n)!}\int\limits_0^\infty [1 - L(u)]u^{2n-1}du \quad (n = 1, 2, \ldots). \tag{16}$$

In view of (14), Eq. (7) can be transformed into the following one:

$$-\int\limits_{-a}^{a} q(x')\ln\frac{|x'-x|}{h}\,dx' = \pi\theta f(x) + \int\limits_{-a}^{a} q(x')\mathcal{F}\Big(\frac{x'-x}{h}\Big)\,dx'. \tag{17}$$

Here we introduced the notation

$$f(x) = w - \frac{x^2}{2R}, \quad \mathcal{F}(t) = \sum_{n=0}^{\infty} d_n t^{2n}. \tag{18}$$

Our approach to the solution of the integral equation (17) is based on the following formula for Chebyshev polynomials of the first kind (Vorovich et al., 1974):

$$-\frac{1}{\pi}\int\limits_{-1}^{1}\frac{T_n(\eta)}{\sqrt{1-\eta^2}}\ln\frac{|y-\eta|}{\lambda}\,d\eta = \begin{cases} \ln 2\lambda, & n = 0, \\ n^{-1}T_n(y), & n = 1, 2, \ldots . \end{cases} \tag{19}$$

First, we replace the functions (18) in terms of the Chebyshev polynomials as

$$f(x) = \Big(w - \frac{a^2}{4R}\Big)T_0(\xi) - \frac{a^2}{4R}T_2(\xi), \tag{20}$$

$$\begin{aligned}\mathcal{F}\Big(\frac{x'-x}{h}\Big) = d_0 &+ \frac{d_1}{2\lambda^2}\Big(T_2(\xi') + T_2(\xi) + 2\Big) + \frac{d_2}{8\lambda^4}\Big\{T_4(\xi') + 4T_2(\xi) + 3 \\ &+ 12(T_2(\xi') + 1)(T_2(\xi) + 1) + T_4(\xi) + 4T_2(\xi) + 3\Big\} + \ldots,\end{aligned} \tag{21}$$

where $\xi = x/a$, $\xi' = x'/a$, and $\lambda = h/a$ is a large parameter.

Now, the substitution of (21) into the integral on the right-hand side of Eq. (17) yields

$$\begin{aligned}\int\limits_{-a}^{a} q(x')\mathcal{F}\Big(\frac{x'-x}{h}\Big)dx' = d_0\mathcal{P} &+ \frac{d_1}{2\lambda^2}(Q_2 + 2\mathcal{P}) + \frac{d_2}{8\lambda^4}(Q_4 + 16Q_2 + 18\mathcal{P}) \\ &+ \frac{d_3}{32\lambda^6}(Q_6 + 36Q_4 + 225Q_2 + 200\mathcal{P}) \\ &+ T_2\Big(\frac{x}{a}\Big)\Big\{\frac{d_1}{2\lambda^2}\mathcal{P} + \frac{d_2}{2\lambda^4}(3Q_2 + 4\mathcal{P}) \\ &+ \frac{15d_3}{32\lambda^6}(2Q_4 + 16Q_2 + 15\mathcal{P})\Big\} \\ &+ T_4\Big(\frac{x}{a}\Big)\Big(\frac{d_2}{8\lambda^4}\mathcal{P} + \frac{3d_3}{16\lambda^6}(5Q_2 + 6\mathcal{P})\Big) \\ &+ T_6\Big(\frac{x}{a}\Big)\frac{d_3}{32\lambda^6}\mathcal{P} + \ldots .\end{aligned} \tag{22}$$

Here we introduced the notation

$$Q_n = \int\limits_{-a}^{a} T_n\Big(\frac{x}{a}\Big) q(x)\, dx \quad (n = 1, 2, \ldots).$$

Thus, in view of (22), the right-hand side of Eq. (17) can be expressed in terms of the constants P, Q_2, Q_4,..., which are integral characteristics of the contact pressure tensity.

Further, following Argatov and Sabina (2013) and applying formula (19) and the orthogonality of the Chebyshev polynomials, we derive the following equations:

$$\begin{aligned}
\mathcal{P} \ln 2\lambda = {} & \theta \int\limits_{-a}^{a} \frac{f(x)}{\sqrt{a^2 - x^2}}\, dx + d_0 \mathcal{P} + \frac{d_1}{2\lambda^2}(Q_2 + 2\mathcal{P}) \\
& + \frac{d_2}{8\lambda^4}(Q_4 + 16Q_2 + 18\mathcal{P}) \\
& + \frac{d_3}{32\lambda^6}(Q_6 + 32Q_4 + 225Q_2 + 200\mathcal{P}) + \ldots, \qquad (23) \\
Q_2 = {} & 2\theta \int\limits_{-a}^{a} \frac{f(x)}{\sqrt{a^2 - x^2}} T_2\Big(\frac{x}{a}\Big) dx + \frac{d_1}{2\lambda^2}\mathcal{P} + \frac{d_2}{2\lambda^4}(3Q_2 + 4\mathcal{P}) \\
& + \frac{15 d_3}{32\lambda^6}(2Q_4 + 16Q_2 + 15\mathcal{P}) + \ldots, \qquad (24) \\
Q_4 = {} & \frac{d_2}{4\lambda^4}\mathcal{P} + \frac{3d_3}{8\lambda^6}(5Q_2 + 6\mathcal{P}) + \ldots, \qquad (25) \\
Q_6 = {} & \frac{3d_3}{32\lambda^6}\mathcal{P} + \ldots . \qquad (26)
\end{aligned}$$

Observe that the asymptotic expansions (22) – (26) contain only the first four asymptotic constants d_0, d_1, d_2, and d_3.

Now, in view of the first formula (18), we will have

$$\int\limits_{-a}^{a} \frac{f(x)}{\sqrt{a^2 - x^2}}\, dx = \pi\Big(w - \frac{a^2}{4R}\Big), \quad \int\limits_{-a}^{a} \frac{f(x)}{\sqrt{a^2 - x^2}} T_2\Big(\frac{x}{a}\Big)\, dx = -\frac{\pi a^2}{8R}. \qquad (27)$$

On the other hand, according to Vorovich et al. (1974), Eq. (18) is equivalent to the integral equation

$$\begin{aligned}
q(x) = {} & \frac{1}{\pi\sqrt{a^2 - x^2}} \Bigg\{ \mathcal{P} - \theta \int\limits_{-a}^{a} \frac{f'(t)\sqrt{a^2 - t^2}}{t - x}\, dt \\
& + \frac{1}{\pi h} \int\limits_{-a}^{a} \frac{\sqrt{a^2 - t^2}}{t - x}\, dt \int\limits_{-a}^{a} q(\xi) \mathcal{F}'\Big(\frac{\xi - t}{h}\Big) d\xi \Bigg\}. \qquad (28)
\end{aligned}$$

Thus, taking into account the asymptotic expansion (21), we derive from Eq. (28) that

$$q(x)=\frac{1}{\pi a\sqrt{1-\xi^2}}\Biggl\{\mathcal{P}+\frac{\pi\theta a^2}{2R}(1-2\xi^2)-\mathcal{P}\Bigl[\varepsilon^2 d_1(1-2\xi^2)$$
$$+\varepsilon^4\frac{d_2}{2}(7-8\xi^2-8\xi^4)+\varepsilon^6\frac{3d_3}{4}(13+6\xi^2-36\xi^4-8\xi^6)\Bigr]$$
$$-Q_2\Bigl(\varepsilon^4 3d_2(1-2\xi^2)+\varepsilon^6\frac{15d_3}{4}(3-8\xi^4)\Bigr)-Q_4\varepsilon^6\frac{15d_3}{8}(1-2\xi^2)+\ldots\Biggr\}, \quad (29)$$

where we introduced the notation $\xi = x/a$ and

$$\varepsilon=\frac{1}{\lambda}=\frac{a}{h}. \quad (30)$$

In view of (24) – (26), formula (29) takes the form

$$q(x)=\frac{1}{\pi a\sqrt{1-\xi^2}}\Biggl\{\mathcal{P}+\frac{\pi\theta a^2}{2R}\Bigl[1-2\xi^2+\varepsilon^4\frac{3d_2}{2}(1-2\xi^2)+\varepsilon^6\frac{15d_3}{8}(3-8\xi^4)\Bigr]$$
$$-\mathcal{P}\Biggl(\varepsilon^2 d_1(1-2\xi^2)+\varepsilon^4\frac{d_2}{2}(7-8\xi^2-8\xi^4)$$
$$+\varepsilon^6\Bigl[\frac{3d_1d_2}{2}(1-2\xi^2)+\frac{3d_3}{4}(13+6\xi^2-36\xi^4-8\xi^6)\Bigr]\Biggr)+\ldots\Biggr\}. \quad (31)$$

The condition that the contact pressure (31) should be equal to zero at the ends of the contact interval implies the following approximate (up to terms of order $O(\varepsilon^8)$) equation:

$$\mathcal{P}\Bigl(1+\varepsilon^2 d_1+\varepsilon^4\frac{9d_2}{2}+\frac{3\varepsilon^6}{4}(2d_1d_2+25d_3)\Bigr)\simeq\frac{\pi\theta a^2}{2R}\Bigl(1+\varepsilon^4\frac{3d_2}{2}+\varepsilon^6\frac{75d_3}{8}\Bigr). \quad (32)$$

Furthermore, in view of (24) – (27), Eq. (23) with the accuracy up to sixth order terms in ε, including, can be written as

$$\mathcal{P}\Bigl\{\ln\frac{2}{\varepsilon}-d_0-\varepsilon^2 d_1-\frac{\varepsilon^4}{4}(d_1^2+9d_2)-\frac{\varepsilon^6}{4}(8d_1d_2+25d_3)\Bigr\}\simeq$$
$$\simeq\pi\theta w-\frac{\pi\theta a^2}{4R}\Bigl(1+\varepsilon^2\frac{d_1}{2}+2\varepsilon^4 d_2+\frac{3\varepsilon^6}{32}(8d_1d_2+75d_3)\Bigr). \quad (33)$$

In turn, taking into account Eq. (33), we can simplify formula (31) as follows:

$$q(x)=\frac{\theta a}{R}\sqrt{1-\xi^2}\Biggl\{1-\varepsilon^2 d_1-\frac{\varepsilon^4}{2}(4d_2\xi^2-2d_1^2+5d_2)$$
$$-\frac{\varepsilon^6}{4}\Bigl(12d_3\xi^4-4(2d_1d_2-9d_3)\xi^2+4d_1^3-22d_1d_2+27d_3\Bigr)\Biggr\}. \quad (34)$$

Note that formula (34) is in agreement with the fourth-order asymptotic solution obtained previously in (Vorovich et al., 1974; Aleksandrov, 2011). Correspondingly, Eqs. (32) and (33) agree with the respective equations in (Vorovich et al., 1974). Finally, formula (31) can be derived from a general result for an arbitrary function $f(x)$ in Eq. (17) obtained by (Aleksandrov, 2006) (see Eq. (3.6) in his work).

4 Asymptotic approximation for the displacement-force relationship

For relating the contact force $P = l\mathcal{P}$ to the indenter displacement w and the contact zone size a, we derived two equations (32) and (33), the first of which is asymptotically equivalent (up to terms of order $O(\varepsilon^8)$) to the following equation:

$$\rho \simeq \varepsilon\Big\{1 - \varepsilon^2\frac{d_1}{2} - \frac{3\varepsilon^4}{8}(4d_2 - d_1^2) - \frac{\varepsilon^6}{16}(75d_3 - 36d_1d_2 + 5d_1^3)\Big\}. \tag{35}$$

Here, in view of (13), we introduced the auxiliary notation

$$\rho = \sqrt{\frac{2RP}{\pi\theta l h^2}}. \tag{36}$$

It is to emphasize that ρ is a dimensionless parameter.

By asymptotically inverting Eq. (35), we obtain

$$\varepsilon \simeq \rho\Big(1 + \rho^2\frac{d_1}{2} + \frac{3\rho^4}{8}(4d_2 + d_1^2) + \frac{\rho^6}{16}(75d_3 + 60d_1d_2 + 5d_1^3)\Big). \tag{37}$$

Now, the substitution of (37) into Eq. (33) yields

$$\begin{aligned}\frac{4Rw}{h^2} \simeq \rho^2\Big\{&2\ln\frac{2}{\rho} - 2d_0 + 1 - \rho^2\frac{3d_1}{2} - \rho^4\Big(d_1^2 + \frac{5d_2}{2}\Big)\\ &-\rho^6\Big(\frac{175}{32}d_3 + \frac{25}{4}d_1d_2 + \frac{5}{6}d_1^3\Big)\Big\}.\end{aligned} \tag{38}$$

Finally, substituting the asymptotic expression (35) into Eq. (38), we arrive at the following relation between the indenter displacement and the relative size of the contact zone:

$$\begin{aligned}\frac{4Rw}{h^2} \simeq \varepsilon^2\Big\{&2\ln\frac{2}{\varepsilon} - 2d_0 + 1 - \varepsilon^2 d_1\Big(2\ln\frac{2}{\varepsilon} + \frac{3}{2} - 2d_0\Big)\\ &+\varepsilon^4\Big(2(d_1^2 - 3d_2)\ln\frac{2}{\varepsilon} + \frac{3d_1^2}{2} - 2d_0d_1^3 - \frac{5d_2}{2} + 6d_0d_2\Big)\Big\}.\end{aligned} \tag{39}$$

Note that the sixth-order asymptotic expansions (35) and (38) allows to obtain also the next asymptotic term in (39). Formula (38) agrees with the zeroth-order asymptotic model developed in (Argatov, 2001) in a more general situation.

In the case of an isotropic layer resting without friction on a rigid foundation (unbonded layer), we have $\theta = 0.5E'$, where $E' = E/(1-\nu^2)$ is the plane strain modulus, E and ν are Young's modulus and Poisson's ratio, respectively. According to Vorovich et al. (1974), the asymptotic constants $d_0, d_1, \ldots$ do not depend on the elastic properties and can be calculated by formulas (15) and (16), where

$$L(u) = \frac{\mathrm{ch}(2u) - 1}{\mathrm{sh}(2u) + 2u}.$$

In this way, one obtains $d_0 = 0.3517$, $d_1 = -0.521$, $d_2 = 0.1349$, and $d_3 = -0.0346$.

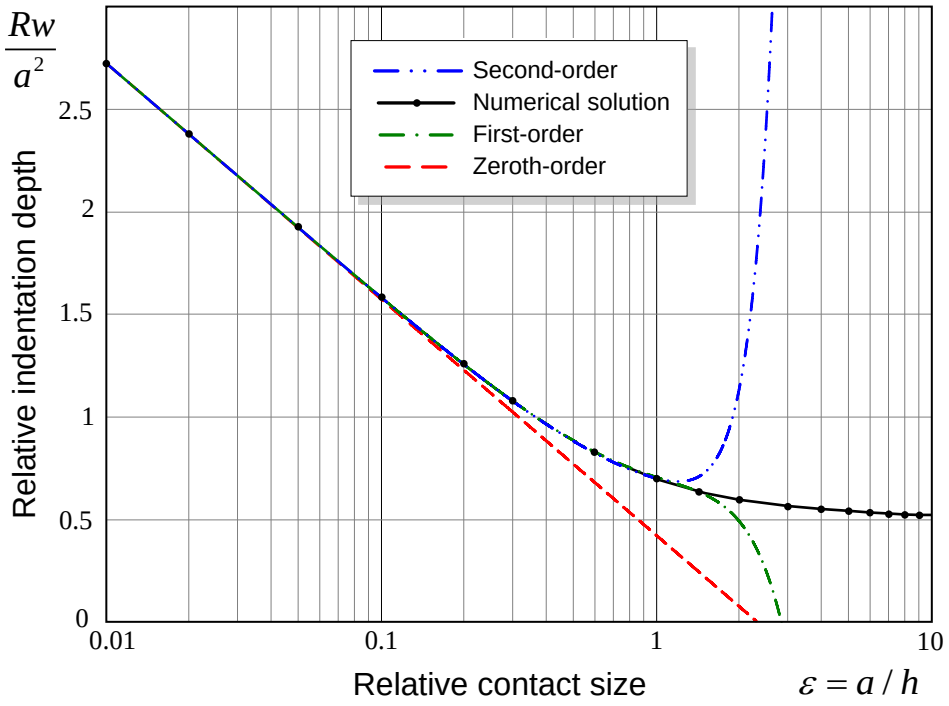

Figure 7. Variation of the relative indenter displacement against the relative size of the contact zone. Comparison with the numerical solution presented by Greenwood and Barber (2012).

Figs. 7 and 8 present the comparison of the numerical solution obtained by Greenwood and Barber (2012) in the isotropic case with the asymptotic approximations based on formulas (39) and (38), respectively. The order of asymptotic approximation is determined by the highest subscript of the asymptotic constants d_0, d_1, d_2, d_3 used in the asymptotic approximation. It was observed (Greenwood and Barber, 2012) that the zeroth-order approximation $Rw = a^2 \ln(2.320h/a)$ is good up to $a/h \approx 0.2$, whereas Fig. 7 shows that the range of validity of the first-order approximation increases up to $a/h \approx 1$. Note also that the forth-order asymptotic solution for the isotropic case was recommended for use in the range $h/a \geq 2$ (Vorovich et al., 1974).

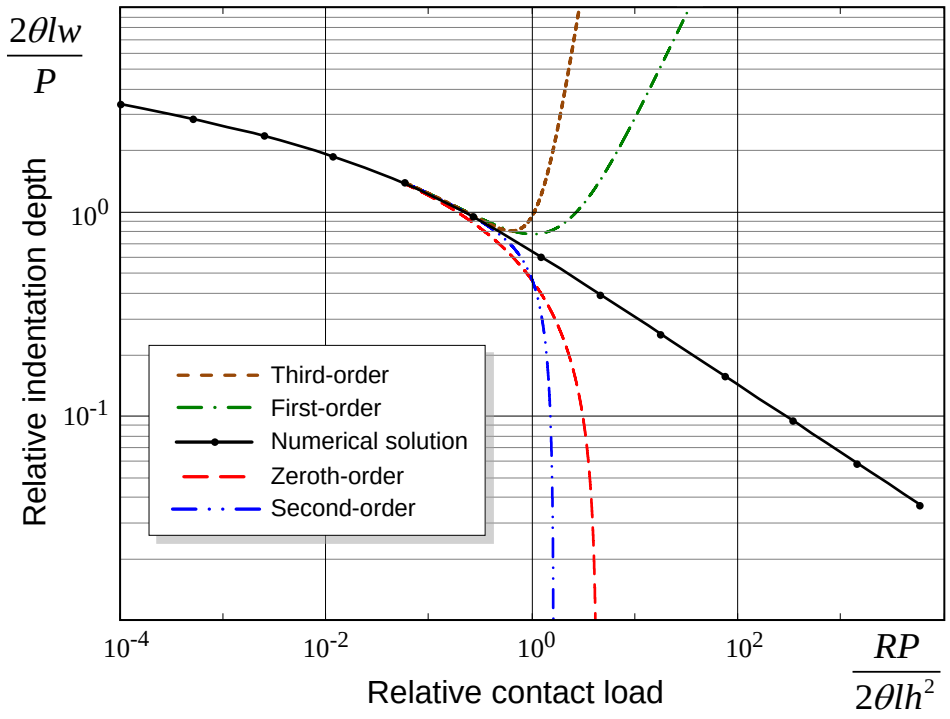

Figure 8. Variation of the relative indenter displacement against the relative contact load. Comparison with the numerical solution presented by Greenwood and Barber (2012).

5 Application to indentation testing

Our depth-sensing indentation method is based on the asymptotic formula (38), which can be rewritten as follows:

$$\frac{w}{w_0} \simeq \frac{P}{P_0}\left\{\ln\frac{P_0}{P} - D_0 - D_1\frac{P}{P_0} - D_2\left(\frac{P}{P_0}\right)^2 - D_3\left(\frac{P}{P_0}\right)^3\right\}. \tag{40}$$

Here we introduced the notation

$$P_0 = \frac{\pi\theta l h^2}{2R}, \quad w_0 = \frac{h^2}{4R}, \quad D_0 = 2d_0 - 1 - 2\ln 2, \tag{41}$$

$$D_1 = \frac{3d_1}{2}, \quad D_2 = d_1^2 + \frac{5d_2}{2}, \quad D_3 = \frac{175}{32}d_3 + \frac{25}{4}d_1d_2 + \frac{5}{6}d_1^3. \tag{42}$$

Observe that while the parameter w_0 is determined solely by the geometry of both the elastic sample and the rigid indenter, the parameter P_0 depends on the elastic constant θ, which, in the case of indentation testing, is not known a priori.

In the longitudinal case (indenter is oriented along the fibers), according to Eqs. (5), (10), (12), and (15), we find that the asymptotic constants $d_0, d_1, \ldots$ are independent of elastic properties of the sample and are evaluated as follows:

$$d_0^{||} = 0.3517, \quad d_1^{||} = -0.521, \quad d_2^{||} = 0.1349, \quad d_3^{||} = -0.0346. \tag{43}$$

At that, the elastic constant entering the first formula (41) is given by

$$\theta^{\|} = \frac{En}{2(n-\nu_{\|}^2)}, \tag{44}$$

where

$$n = \frac{E_{\|}}{E}. \tag{45}$$

The obtained analytical solution in the longitudinal case are illustrated by Figs. 9 and 10. These figures differ by the choice of the independent variable: the contact zone size (Fig. 9) and the indenter displacement (Fig. 10).

It should be emphasized that because formula (40) was obtained under the assumption of small contact, the indentation depth w should be relatively small compared with the sample thickness h. The last condition depends also on the indenter radius R and is governed by the dimensionless quantity $4Rw/h^2$ (see Eq. (39)). This is shown with an illustrative example of a relative indentation depth of 20% in Fig. 9.

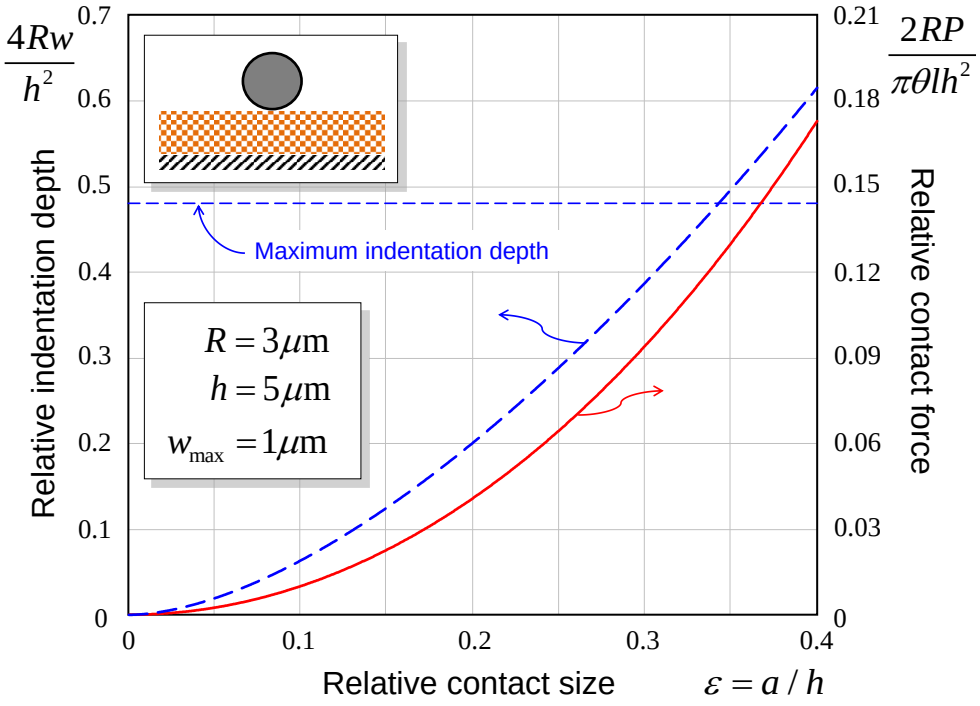

Figure 9. Variation of the indenter displacement (dashed line) and the contact force (solid line) against the size of the contact zone in the longitudinal case.

In the transverse case (indenter is perpendicular to the fibers), formulas (6) can be rewritten as

$$A^{\perp} = \frac{n(n-m\nu_{\|})(1+\nu)}{m(n-\nu_{\|}^2)}, \quad B^{\perp} = \frac{n^2(1-\nu^2)}{n-\nu_{\|}^2}, \tag{46}$$

where

$$m = \frac{G_{\|}}{G} = \frac{2(1+\nu)G_{\|}}{E}. \tag{47}$$

It is to note that the relationship between $(A^{\perp})^2$ and $B^{\perp}$, and correspondingly the choice of the kernel function $L(u)$ from formulas (9) and (11), depends on the values of Poisson's

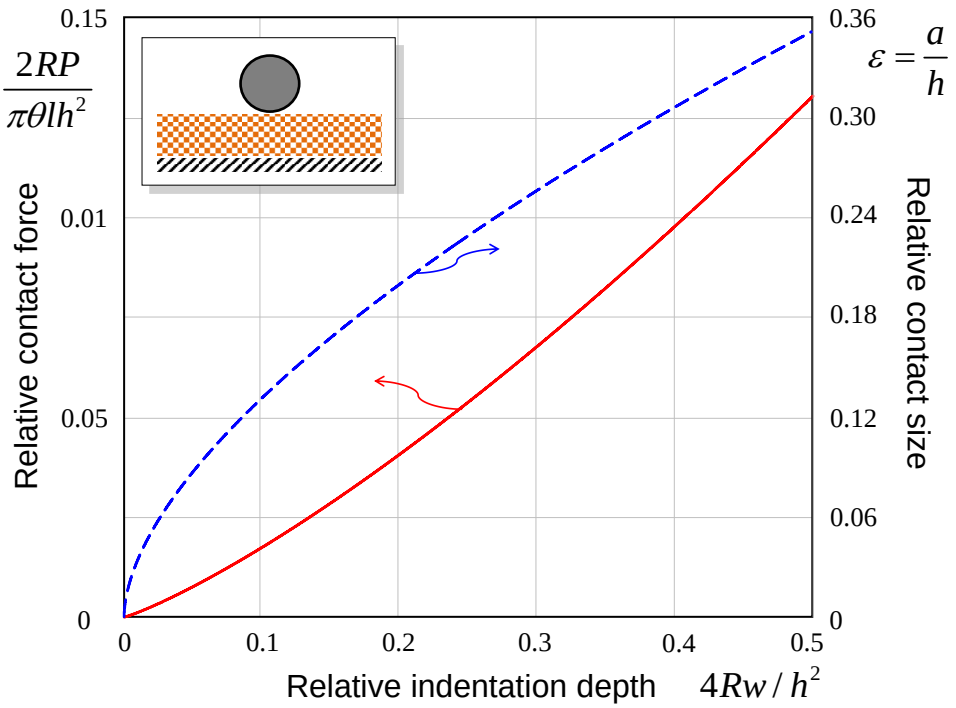

Figure 10. Variation of the contact force (solid line) and the contact zone size (dashed line) against the indenter displacement in the longitudinal case.

ratios ν and $\nu_{\|}$ as well as on the values of the elastic moduli ratios n and m. At the same time, it should be emphasized that the values of the asymptotic constants $d_0, d_1, \ldots$ also depend on the normalization of $L(u)$ through the choice of the elastic constant θ (see Eqs. (7) and (8) derived by Aleksandrov (2006)). Because a continuous shift in d_0 and d_n is required when solving the inverse problem of material parameter identification, the following new normalization is adopted:

$$L(u) = \begin{cases} \dfrac{\kappa_1 + \kappa_2}{2\kappa_1\kappa_2} L_+(u) & (A^2 > B), \\ \dfrac{1}{A} L_0(u) & (A^2 = B), \\ \dfrac{c}{c^2 + d^2} L_-(u) & (A^2 < B). \end{cases} \tag{48}$$

At that, the corresponding elastic constant θ in Eqs. (8), (17), (36), and (41) is evaluated as

$$\theta = \frac{\gamma}{2}, \tag{49}$$

where the value of γ is given by (12).

Further, recall that even in the isotropic case, the evaluation of Young's modulus of an elastic sample by frictionless indentation, generally speaking, requires the knowledge of Poisson's ratio of the sample (Fischer-Cripps, 2004). Accordingly, we will assume that Poisson's ratios ν and $\nu_{\|}$ are known in advance, and the problem of material parameters identification reduces to the evaluation of three elastic constants E, $E_{\|}$, and $G_{\|}$.

It is clear that, because the asymptotic constants (43) are independent of the material properties, in the longitudinal case, fitting the experimental data for the force-displacement relationship with the analytical approximation (40) allows to determine

only one elastic constant $\theta^{||}$.

In the transverse case, by fitting the experimental depth-load data with the analytical approximation (40), one can determine the elastic constants n, m, and

$$\theta^{\perp} = \frac{2R}{\pi l h^2} P_0^{\perp}, \tag{50}$$

where $P_0^{\perp}$ is the corresponding best-fit value for P_0 in (40).

Thus, in view of (12), we obtain

$$E = 2(1-\nu^2)\theta^{\perp}, \quad E_{\|} = nE, \quad G_{\|} = \frac{mE}{2(1+\nu)}. \tag{51}$$

Formulas (50) and (51) solve the formulated above material properties identification problem.

6 Application to indentation testing of a collagen layer

To illustrate the outlined identification procedure, we consider the cylindrical lateral depth-sensing indentation of a collagen coating freely deposited on a glass substrate with the fibril direction perpendicular to the cylinder axis (see Fig. 5). The collagen membrane thickness is approximately 5 μm. The indenter cylinder length is about 18 μm, and the cylinder diameter is 6 μm.

In particular, the experimental data was fitted with the following three approximations:

$$\bar{w} = -\bar{P}(\ln \bar{P} + D_0), \tag{52}$$

$$\bar{w} = -\bar{P}(\ln \bar{P} + D_0 + D_1\bar{P}), \tag{53}$$

$$\bar{w} = -\bar{P}(\ln \bar{P} + D_0 + D_1\bar{P} + D_2\bar{P}^2). \tag{54}$$

Here, $\bar{w} = w/w_0$ and $\bar{P} = P/P_0$.

Correspondingly, under the assumption that $\nu = \nu_{\|} = 0.45$, the following best-fit values were obtained: $\theta_0^{\perp} = 8.94$ MPa, $n_0 = 6.63$, $m_0 = 1.40$ for (52), $\theta_1^{\perp} = 10.60$ MPa, $n_1 = 8.25$, $m_1 = 1.05$ for (53), and $\theta_2^{\perp} = 10.42$ MPa, $n_2 = 8.19$, $m_2 = 1.06$ for (54). Now, using the first two formulas (51), we get three approximations for the longitudinal elastic modulus as follows: $E_{\|}^0 = 94.6$ MPa, $E_{\|}^1 = 139.6$ MPa, and $E_{\|}^2 = 136.2$ MPa.

Fig. 11 shows the obtained results for the approximations (53) and (54) only, because the curve corresponding to the approximation (52) almost coincides with that for (53) (with the maximum relative difference of 10% near the beginnning of the scale). It can be seen that while the use of the zero-order approximation (52) with only one asymptotic constant d_0 is not enough for accurate identification, the increase of the number of the asymptotic constants from two (d_0 and d_1) to three (d_0, d_1, and d_2) reduces the robustness of the best square fit procedure. Note that in the longitudinal case, when the coefficients

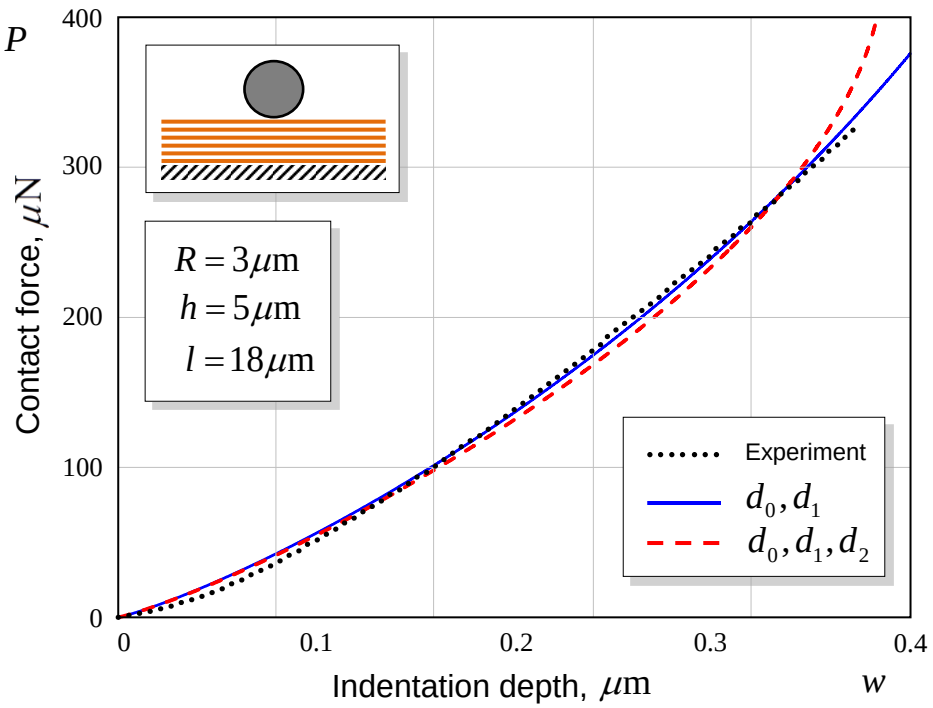

Figure 11. Depth-sensing indentation data best-fitted with the approximations (53) (solid line) and (54) (dashed line).

of the approximation (40) are independent of the material properties, by formulas (42) and (43), we obtain $D_1^{||} = -0.782$, $D_2^{||} = 0.609$, and $D_3^{||} = -0.747$ so that the absolute values of the coefficients D_j, it seems, do not decay with the subscript 'j'. On the other hand, it was observed previously (Andrianov et al., 2003; Argatov, 2011) that the range of applicability of asymptotic formulas reduces, while their accuracy increases. That is why, because in real indentation tests, the relative size of the contact zone is not sufficiently small, the practical application of formula (53) is recommended.

7 Discussion and conclusions

It should be emphasized that formulas (9) – (11) hold true only in the case of frictionless bilateral contact between a transversely isotropic elastic layer and a rigid substrate.

At the same time, the asymptotic solution obtained in Section 3 will be also valid in the case of an elastic layer attached to a rigid substrate, provided the corresponding solution is obtained for the kernel function $L(u)$ in (10).

The proposed indentation material parameters identification method utilizes the depth-load indentation data for the cylinder indenter oriented orthogonal to the fiber direction only. If the depth-load data are available for the other indenter position (along the fiber direction), they can be used for verifying the predicted value of the transverse modulus E.

Finally, we would like to emphasize that the proposed material identification method has several limitations (some of them were discussed previously). In particular, both Poisson's

ratios must either be assumed — as it is often the case in the indentation testing of biological materials (Ebenstein and Pruitt, 2006) — or determined a priori by a secondary different type of test. In the three-dimensional case of an isotropic elastic layer, Jin and Lewis (2004) developed an approach, which utilizes different-sized flat-ended cylindrical indenters. However, as far as we know, the extension of this method to other indenter configurations as well as to the case of material anisotropy is an open question.

Recall that the constructed asymptotic solution assumes that the contact zone size, a, is small compared to the elastic film thickness, h. On the other hand, the film thickness h should be small compared to the cylinder indenter length, l, in order to apply a two-dimensional approximation for the stress-strain state beneath the indenter. We emphasize that while the ratio h/l is determined solely by the film and indenter characteristic sizes, the ratio a/h depends on the indentation depth (see Fig. 9).

In the present paper, the sixth-order asymptotic model for the frictionless unilateral contact of a cylindrical indenter is constructed in the framework of the two-dimensional elasticity theory. Explicit asymptotic formulas are derived in Section 4 for the relationship between the load and the contact size (see formulas (35) and (37)) as well as for the relations of the indenter displacement to the contact load (see formula (38)) and to the contact size (see formula (39)). The results obtained can be applied for the development of cylindrical lateral indentation tests for elastic samples thin compared to the cylinder indenter length.

8 Acknowledgment

The authors are very grateful to Yuri Bobrov and Marko Surtchev (NT-MDT) for the AFM measurements and technical support. GM also acknowledges support from the FP7 IRSES Marie Curie grant TAMER No 610547R.

References

Aleksandrov, V.M., 2006. Two problems with mixed boundary conditions for an elastic orthotropic strip. J. Appl. Math. Mech. 70, 128–138.

Aleksandrov, V.M., 2011. The integral equations of plane contact problems for high values of the parameter. J. Appl. Math. Mech. 75, 711–715.

Andrianov, I.V., Awrejcewicz, J., Barantsev, R.G., 2003. Asymptotic approaches in mechanics: new parameters and procedures. Appl. Mech. Rev. 56, 87–110.

Argatov, I.I., 2001. Solution of the plane Hertz problem. J. Appl. Mech. Tech. Phys. 42, 1064–1072.

Argatov, I.I., 2010. Frictionless and adhesive nanoindentation: Asymptotic modeling of size effects. Mech. Mater. 42, 807–815.

Argatov, I.I., 2011. Depth-sensing indentation of a transversely isotropic elastic layer: Second-order asymptotic models for canonical indenters. Int. J. Solids Struct. 48, 3444–3452.

Argatov, I., Daniels, A.U., Mishuris, G., Ronken, S., Wirz, D., 2013. Accounting for the thickness effect in dynamic spherical indentation of a viscoelastic layer: Application to non-destructive testing of articular cartilage. Eur. J. Mech. A/Solids 37, 304–317.

Argatov, I.I., Sabina, F.J., 2013. Asymptotic analysis of the substrate effect for an arbitrary indenter. Quart. J. Mech. Appl. Math. 66, 75–95.

Batra, R.C., Jiang, W., 2008. Analytical solution of the contact problem of a rigid indenter and an anisotropic linear elastic layer. Int. J. Solids Struct. 45, 5814–5830.

Borodich, F.M., Keer, L.M., Korach, Ch.S., 2003. Analytical study of fundamental nanoindentation test relations for indenters of non-ideal shapes. Nanotechnology 14, 803–808.

Choi, S.T., Jeong, S.J., Earmme, Y.Y., 2008. Modified-creep experiment of an elastomer film on a rigid substrate using nanoindentation with a flat-ended cylindrical tip. Scripta Mater. 58, 199–202.

Delafargue, A., Ulm, F.-J., 2004. Explicit approximations of the indentation modulus of elastically orthotropic solids for conical indenters. Int. J. Solids Struct. 41, 7351–7360.

Dimitriadis, E.K., Horkay, F., Maresca, J., Kachar, B., Chadwick, R.S. 2002. Determination of elastic moduli of thin layers of soft material using the atomic force microscope. Biophys. J. 82, 2798–2810.

Ding, H.J., Chen, W.Q., Zhang, L., 2006. Elasticity of Transversely Isotropic Materials, Dordrecht, Springer.

Ebenstein, D.M., Pruitt, L.A., 2006. Nanoindentation of biological materials. Nanotoday 1, 26–33.

Erbaş, B., Yusufoğlu, E., Kaplunov, J., 2011. A plane contact problem for an elastic orthotropic strip. J. Eng. Math. 70, 399–409.

Fischer-Cripps, A.C., 2004. Nanoindentation, New York, Springer-Verlag.

Giannakopoulos, A.E., 2006. Elastic and viscoelastic indentation of flat surfaces by pyramid indentors. J. Mech. Phys. Solids 54, 1305–1332.

Greenwood, J.A., Barber, J.R., 2012. Indentation of an elastic layer by a rigid cylinder. Int. J. Solids Struct. 49, 2962–2977.

Hayes, W.C., Keer, L.M., Herrmann, G., Mockros, L.F., 1972. A mathematical analysis for indentation tests of articular cartilage. J. Biomech. 5, 541–551.

Huang, N.F., Okogbaa, J., Lee, J.C., Jha, A., Zaitseva, T.S., Paukshto, M.V., Sun, J.S., Punjya, N., Fuller, G.G., Cooke, J.P., 2013. The modulation of endothelial cell morphology, function, and survival using anisotropic nanofibrillar collagen scaffolds. Biomater. 34, 4038–4047.

Jin, H., Lewis, J.L., 2004. Determination of Poisson's ratio of articular cartilage by indentation using different-sized indenters. J. Biomech. Eng. 126, 138–145.

Korhonen, R.K., Saarakkala, S., Töyräs, J., Laasanen, M.S., Kiviranta, I., Jurvelin, J.S., 2003. Experimental and numerical validation for the novel configuration of an arthroscopic indentation instrument. Phys. Med. Biol. 48, 1565–1576.

Lekhnitskii, S.G. 1981. Theory of Elasticity of an Anisotropic Body. Mir publishing, Moscow.

Liao, Q., Huang, J., Zhu, T., Xiong, C., Fang, J., 2010. A hybrid model to determine mechanical properties of soft polymers by nanoindentation. Mech. Mater. 42, 1043–1047.

Nayak, L., Johnson, K.L., 1979. Pressure between elastic bodies having a slender area of contact and arbitrary profiles. Int. J. Mech. Sci. 21, 237–247.

Pandolfi, A., Vasta, M., 2012. Fiber distributed hyperelastic modeling of biological tissues. Mech. Mater. 44, 151–162.

Pelletier, H., Krier, J., Mille, P., 2006. Characterization of mechanical properties of thin films using nanoindentation test. Mech. Mater. 38, 1182–1198.

Stolz, M., Gottardi, R., Raiteri, R., Miot, S., Martin, I., Imer, R., Staufer, U., Raducanu, A., Düggelin, M., Baschong, W., Daniels, A.U., Friederich, N.F., Aszodi, A., Aebi, U., 2009. Early detection of aging cartilage and osteoarthritis in mice and patient samples using atomic force microscopy. Nature Nanotech. 4, 186–192.

Sveklo, V.A., 1964. Boussinesq type problems for the anisotropic half-space. J. Appl. Math. Mech. 28, 1099–1105.

Vlassak, J.J., Ciavarella, M., Barber, J.R., Wang, X., 2003. The indentation modulus of elastically anisotropic materials for indenters of arbitrary shape. J. Mech. Phys. Solids 51, 1701–1721.

Vlassak, J.J., Nix, W.D., 1993. Indentation modulus of elastically anisotropic half spaces. Phil. Mag. A 67, 1045–1056.

Vlassak, J.J., Nix, W.D., 1994. Measuring the elastic properties of anisotropic materials by means of indentation experiments. J. Mech. Phys. Solids 42, 1223–1245.

Vorovich, I.I., Aleksandrov, V.M., Babeshko, V.A., 1974. Non-classical Mixed Problems of the Theory of Elasticity. Nauka, Moscow [in Russian].

Willis, J.R., 1966. Hertzian contact of anisotropic bodies. J. Mech. Phys. Solids 14, 163–176.

Willis, J.R., 1967. Boussinesq problems for an anisotropic half-space. J. Mech. Phys. Solids 15, 331–339.